

Growth of Rh, Pd, and Pt films on Cu(100)

G. W. Graham

Research Staff, Ford Motor Company, Dearborn, Michigan 48121

P. J. Schmitz and P. A. Thiel

Department of Chemistry and Ames Laboratory, Iowa State University, Ames, Iowa 50011

(Received 28 September 1989)

The growth of vapor-deposited films of Rh, Pd, and Pt on Cu(100) at 300 K was followed by Auger-electron and low-energy ion scattering spectroscopies. A tendency (strong for Rh, weaker for both Pd and Pt) for Cu to remain on the surface as the film grows was observed, consistent with expectations based on surface energy considerations. The much smaller difference in behavior between Pt and Pd than between Pt and Rh can be related to the heat of mixing, the sign of which is positive for Cu-Rh but negative for both Cu-Pd and Cu-Pt. While agglomeration does not appear to be significant, the experimental results suggest that a fraction of the deposited metal forms clusters, islands, or other configurations which are relatively stable against the surface diffusional processes thought to be responsible for incorporation of adatoms into the bulk. The ordered 50-50 surface alloy phase previously found for Pd on Cu(100) was not observed in the case of Pt, although a $c(2 \times 2)$ low-energy electron-diffraction pattern is produced by the nearly pure Cu surface which results from heating a monolayer (deposited) of either metal to 450 K. Photoemission and chemisorption results reveal other differences among the three combinations of metals.

I. INTRODUCTION

Metal epitaxy has been studied extensively.¹ The basic growth modes, for example, were sorted out by Bauer more than 30 years ago.² Nevertheless, it remains of interest to develop a detailed understanding of the factors involved in the growth of metal films. This interest is derived from work on artificial multilayer materials as well as studies of electronic and/or magnetic modifications in ultrathin films. In both instances, the desired film-substrate combination may be one for which uniform film growth is not expected under the quasiequilibrium conditions assumed by Bauer. The conditions required to achieve kinetically limited growth and ultimately preserve a metastable configuration are generally not known since relatively few such film-substrate combinations have been thoroughly investigated.

An example of just such a system is Rh on Ag(100).³ Since the surface energy of Rh is more than twice that of Ag (and Rh is essentially insoluble in Ag), growth of three-dimensional Rh crystallites (Volmer-Weber mode) might be anticipated. In fact, statistical layer-by-layer growth (pseudo-Frank-van der Merwe mode) was found at a substrate temperature of 300 K, presumably because agglomeration of Rh into three-dimensional crystallites is a relatively slow process at this temperature. At higher temperature, 600 K, growth was again found to be roughly layer by layer, though in a lower-energy configuration in which about 1 monolayer (ML) of Ag covered the Rh (or Rh-rich) film. This behavior is understood to result from the larger thermal energy available for atomic rearrangement at 600 K than at 300 K together with a sufficiently defective film structure to allow rapid Ag diffusion to the free surface of the growing Rh film. The

driving force for this diffusion, a substantial lowering of the surface energy, exists as long as the Rh surface is bare.

In the present work, film growth of the three metals, Rh, Pd, and Pt, on Cu(100) at 300 K is compared. The behavior of Rh on Cu(100) appears to be rather similar to that of Rh on Ag(100), except that rapid diffusion of Cu to the surface of the Rh film occurs even at 300 K. (This difference may reflect the moderate solubility of Rh in Cu.) On the other hand, the tendency for Cu to remain on the surface during the growth of Pd or Pt films is much smaller. There is, in fact, a close similarity between the behaviors of Pd and Pt, contrasted with that of Rh, in spite of the surface-energy differences (J/m^2),⁴ 0.11 for (Pd)-(Cu), 0.76 for (Pt)-(Cu), and 0.89 for (Rh)-(Cu), which would suggest that Pt should behave more like Rh than Pd. The heats of formation (kJ/mol),⁵⁻¹⁴ -14 for CuPd, -10 for CuPt, and +2 for CuRh, emphasize an important qualitative difference between Pt (or Pd) and Rh in terms of their interaction with Cu, however. The difference between the film-growth behaviors of Rh and Pt (or Pd) on Cu can thus be related to the tendency to cluster (Cu-Rh) as opposed to mix (Cu-Pt or Cu-Pd) upon alloy formation.

II. EXPERIMENTAL RESULTS

The experiments were carried out in an ultrahigh-vacuum chamber equipped with shuttered Rh, Pd, and Pt evaporation sources of the electron-bombardment variety, apertured double-pass cylindrical mirror analyzer (CMA) with coaxial electron gun, off-axis electron gun, ion gun, uv lamp, low-energy electron-diffraction (LEED) optics, precision sample manipulator,

and provisions for gas exposure. (Further details of the apparatus may be found in Ref. 6.) Some x-ray photoelectron spectroscopy (XPS) measurements were performed in another similar chamber equipped with an Al $K\alpha$ x-ray source. Base pressures were below 10^{-10} Torr.

The Cu(100) substrate, also used in previous studies,^{6,7} was cleaned by repeated cycles of argon-ion bombardment (2 keV, $4 \mu\text{A}/\text{cm}^2$), first at 300 K and then at 650 K, followed by further heating at 650 K in vacuum. Temperature was measured with a Chromel-Alumel thermocouple clamped against the substrate holder.

Deposition of Rh, Pd, or Pt onto Cu(100) was performed by exposing the substrate at 300 K to flux from the appropriate evaporation source. The associated pressure rise was typically $(2-4) \times 10^{-10}$ Torr for Rh and Pt, and $(8-16) \times 10^{-10}$ Torr for Pd, depending on the duration of the deposition. Auger-electron spectroscopy (AES) was used to monitor surface composition and verify that the deposition rates remained constant over the course of the experiments.

A plot of the peak-to-peak amplitudes of the derivative spectra of the Cu $M_{2,3}VV$ (57 and 60 eV), Cu $L_3M_{4,5}M_{4,5}$ (920 eV), and Rh $M_{4,5}N_{4,5}N_{4,5}$ (302 eV) Auger transitions as a function of total deposition time for a series of sequential depositions is shown in Fig. 1. Assuming layer-by-layer growth, a rough estimate of the Rh deposi-

tion rate (based on exponential variation of the AES signals with a mean free path of 8 Å at 60 eV and 10 Å at 920 eV) is 1 ML in ~ 240 s. A similar plot was obtained for Pd. The Pd deposition rate, 1 ML in ~ 360 s, derived in the same manner, is consistent with a previously reported estimate based on an alternate means of calibration.⁷ The Pt deposition rate, obtained by comparison with AES results from "Cu(100)-c(2×2)Au,"⁶ is 1 ML in ~ 300 s.

LEED patterns were monitored periodically in the course of depositing the metals. In the case of Rh, the pattern was found to evolve from a sharp $p(1 \times 1)$ with low background intensity for clean Cu(100) to a diffuse $p(1 \times 1)$ with high background intensity after 960 s of deposition (~ 4 ML of Rh). In the case of Pd, a good $c(2 \times 2)$ pattern was observed after 300 s of deposition (~ 0.8 ML of Pd), as previously reported.⁷ With further deposition of Pd, the $c(2 \times 2)$ spots were observed to fade, while the background intensity increased continuously. In the case of Pt, the pattern was found to evolve to a diffuse $p(1 \times 1)$ with high background intensity after 960 s of deposition (~ 3 ML of Pt). Faint, diffuse $c(2 \times 2)$ spots were also observed over a narrow range of beam energy near 130 eV after 240 s of deposition (~ 0.8 ML of Pt); at much larger coverages these spots were not apparent, though possibly because of the high background intensity.

The ion-scattering spectroscopy (ISS) measurements were performed by backfilling the vacuum chamber with He to a pressure of 2×10^{-6} Torr and using the apertured CMA (with appropriate potentials reversed) to analyze ions of 1 keV initial kinetic energy which had been scattered through an angle of 147° . The ions were incident on the sample at an angle of 66° with respect to the sample normal. Spectra obtained with the incident beam oriented along different azimuths of the substrate were found to be roughly proportional, implying that the detected ions were just scattered from the outermost atomic layer. Beam-induced damage was not evident.

A series of ion-scattering spectra for Rh on Cu(100), each labeled by the total Rh deposition time, is shown in Fig. 2. The concentration of Cu in the outermost layer is clearly much larger than would be expected on the basis of the AES results for layer-by-layer growth. Heating the sample to 525 K was found to result in an even larger Cu concentration in the outermost layer as shown by the spectrum labeled (a) in Fig. 2. The temperature range over which this change took place, determined by monitoring the Rh scattering-peak amplitude while heating at a rate of $\sim 1\text{K}/\text{s}$, is centered near 425 K and is ~ 60 K wide as shown in Fig. 3. For shorter deposition times the range was found to be centered at lower temperatures, while for longer times it was centered at somewhat higher temperatures, the overall variation being on the order of 10 K.

Ion-scattering spectra were also obtained for Pd and Pt on Cu(100). In both cases, the concentration of Cu in the outermost atomic layer was found to be larger than would be expected on the basis of the AES results for layer-by-layer growth, although to a much smaller extent than for Rh. In addition, heating to 525 K was found to

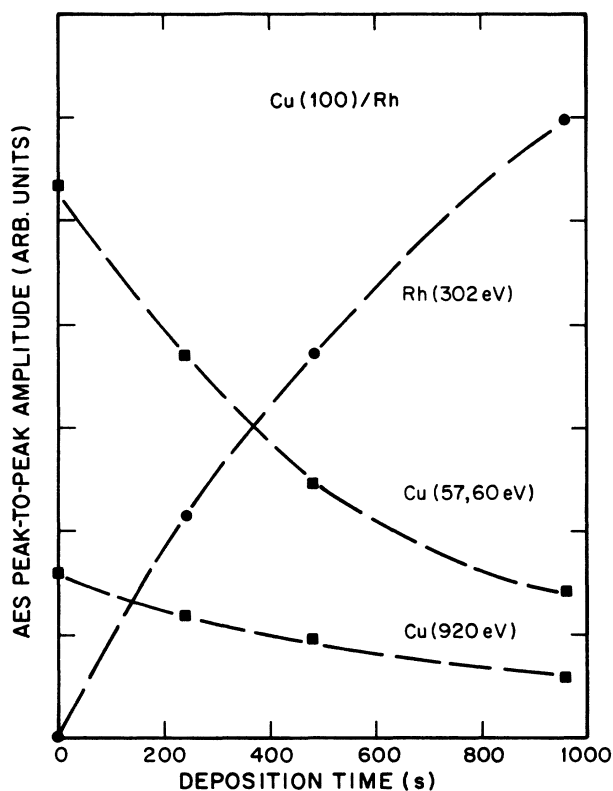


FIG. 1. AES peak-to-peak amplitudes [$dN(E)E/dE$ mode, 4 eV peak-to-peak modulation] as a function of Rh deposition time on Cu(100) at 300 K. The off-axis electron gun, incident at 71° from the sample normal, was operating at 2 keV; the sample normal was parallel to the CMA axis.

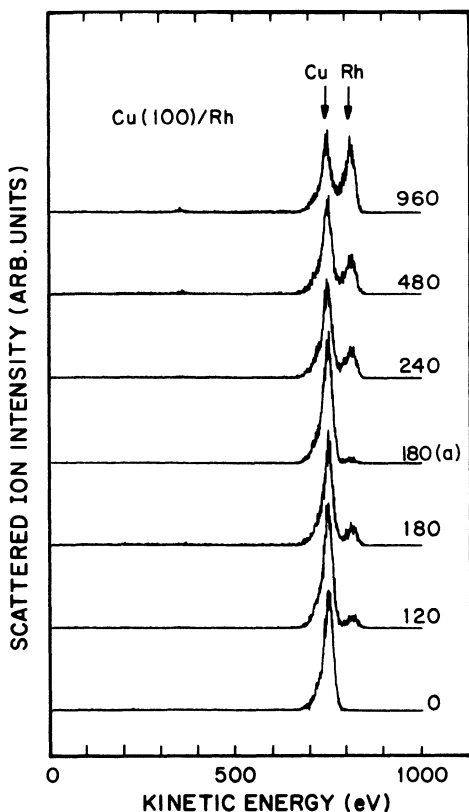


FIG. 2. Ion-scattering spectra from Rh on Cu(100). Numbers labeling the spectra are deposition times in seconds. All spectra are from the as-deposited state (300 K substrate temperature) except for the one labeled (a) which was taken after heating the sample to 525 K. The small peak near 350 eV (most apparent in the top two spectra) is due to CO adsorbed from the residual gas.

result in a larger Cu concentration in the outermost layer, the change taking place over essentially the same temperature range as for Rh. The ISS results for all three systems are compared in Fig. 4 where the scattering-peak amplitudes for Cu in the as-deposited states and the ratios of the scattering-peak amplitudes of the deposited metal to Cu in both the as-deposited states, as well as after heating to 525 K, are plotted as a function of nominal coverage. The ratios of the scattering-peak amplitudes of Rh or Pd to Cu were found to be consistent with calculated atomic-scattering cross sections.⁸ In the case of Pt, however, the ratio in the as-deposited state was found to be smaller than expected, possibly due to some selective adsorption of residual gas. The bend in the Cu plot at 1 ML for the as-deposited state in the case of Pd corresponds to the break in the AES plots reported previously.⁷ It is evidently related to the completion of the structure responsible for the $c(2 \times 2)$ LEED pattern, which was found to be optimum (most intense) near this coverage.^{7,9}

The effect of heating was found to be much less dramatic on the AES than on the ISS results, apparently because of the lower surface sensitivity of AES. In the case of Rh, for example, the AES signals after heating to

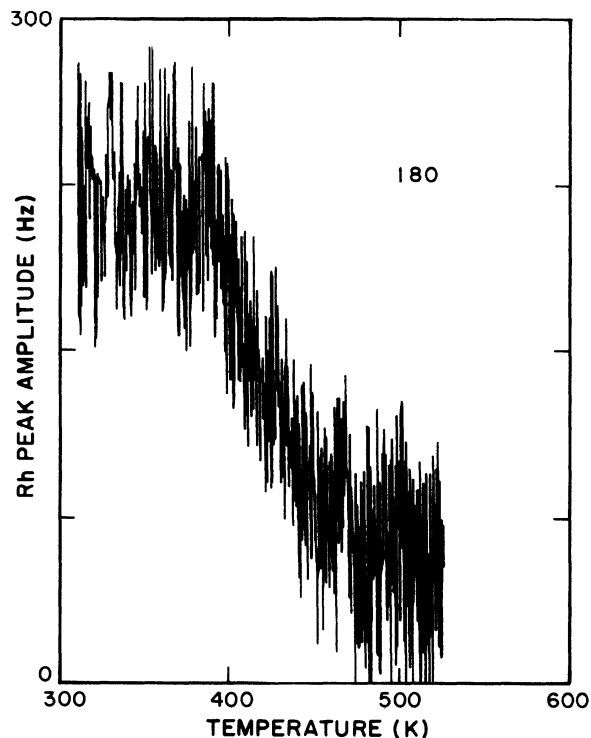


FIG. 3. Rh scattering-peak amplitude as a function of sample temperature while heating Rh (180 s of deposition) on Cu(100) at a rate of ~ 1 K/s.

525 K typically had changed by no more than 5–10 %, always in the direction of larger Cu concentration on the surface, as indicated by ISS.

LEED observations after heating to 525 K revealed some other changes, however. Faint, diffuse $c(2 \times 2)$ spots and streaks along surface $\langle 110 \rangle$ directions were found for Rh (180 s of deposition), while a good $c(2 \times 2)$ pattern was observed for both Pd and Pt (300 and 240 s of deposition, respectively). In the case of Pt, the formation of the $c(2 \times 2)$ spots during the heating was observed to coincide with the change in Cu concentration in the outermost layer, centered near a temperature of 430 K at this coverage. A fainter $c(2 \times 2)$ pattern was also found after heating with half of this Pt coverage, while a diffuse $p(1 \times 1)$ pattern together with broad streaks along surface $\langle 110 \rangle$ directions was found after heating with twice this Pt coverage.

Angle-resolved ultraviolet-photoelectron-spectroscopy (UPS) results for all three systems are shown in Fig. 5. The spectra are again labeled by the deposition times, and those labeled (a) indicate the effect of heating to 525 K. Differences among the three systems in the spectral region just below the Fermi level tend to become smaller as nominal coverages begin to exceed to 1 ML.

Finally, the Pd $3d$ core-level spectrum from Cu(100)- $c(2 \times 2)$ Pd (corresponding to ~ 300 s of Pd in the as-deposited state) is shown in Fig. 6 together with spectra from a thick (~ 50 Å) film of Pd on Cu(100) and an alloy, $\text{Cu}_{1+x}\text{Pd}_{1-x}$ with $x \approx 0.3$ (according to AES and XPS), formed by heating the thick film of Pd on Cu(100) to 715

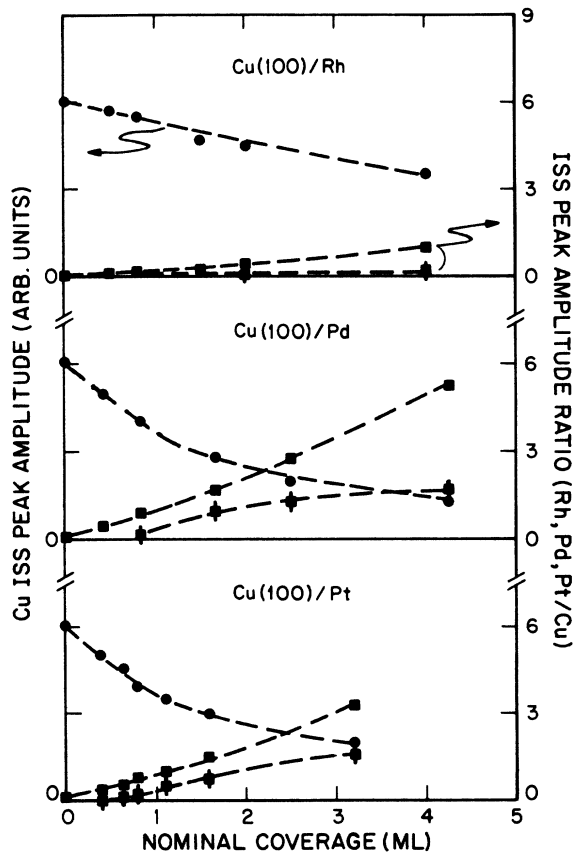


FIG. 4. Cu scattering-peak amplitudes in the as-deposited states (●) and the ratios of the deposited-metal scattering-peak amplitudes to Cu scattering-peak amplitudes in both the as-deposited states (■) as well as after heating to 525 K (■) as a function of nominal coverage.

K. These results have bearing on the issue of absolute coverage calibration as discussed below.

III. DISCUSSION

Since many of the inferences about the film-growth behavior depend on knowledge of the amount of metal deposited, it is worth reviewing the determination of coverages described above.

First of all, the rough estimate of Rh coverage obtained from the AES results was based on assumptions which are clearly flawed since the ISS results indicate that more than half of the surface atoms are Cu after 4 ML of Rh have been deposited. Growth of isolated Rh particles on top of the Cu is ruled out, however, by the approximately exponential approach of the AES signals toward the appropriate asymptotes as expected for layer-by-layer growth. (For 8 ML of deposited Rh the Cu AES signals were found to be less than 10% of their initial values. Moderate amounts of CO were also found on the Rh at this point, however.) It seems likely, instead, that the film grows in a mode similar to that found for Rh deposited on Ag(100) at 600 K.³ The actual Rh coverage

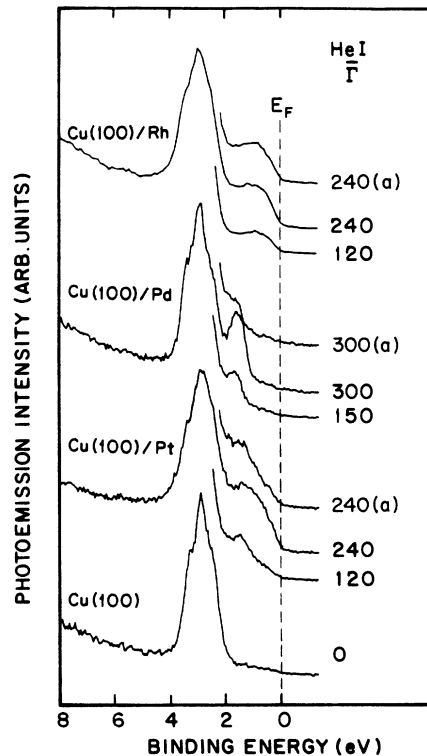


FIG. 5. He I-excited photoelectron spectra from Rh, Pd, and Pt on Cu(100) for emission within 6° of the surface normal at 0.15 eV resolution. Numbers labeling the spectra are deposition times in seconds. All spectra are from the as-deposited state (300 K substrate temperature) except for those labeled (a), which were taken after heating the sample to 525 K.

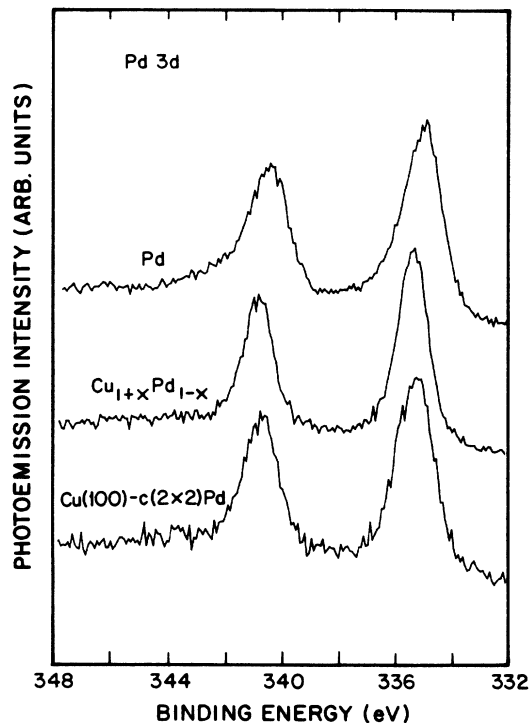


FIG. 6. Pd 3d core-level spectra from a thick ($\sim 50 \text{ \AA}$) layer of Pd on Cu(100), $\text{Cu}_{1+x}\text{Pd}_{1-x}$ with $x \approx 0.3$, and $\text{Cu}(100)\text{-}c(2 \times 2)\text{Pd}$.

would thus be somewhat larger than that estimated.

The situation in the case of Pd is more certain since previous measurements from Pd on W(110) provide an accurate calibration of the deposition rate from the Pd source.¹⁰ In addition, deposition of Pd onto Cu(100) is known to form an ordered 50-50 surface alloy, Cu(100)-*c*(2×2)Pd, at a Pd coverage in the range 0.5–0.8 ML.^{7,9} This knowledge of the Pd coverage together with the apparent similarity between the AES results from Cu(100)/Pd and Cu(100)/Rh suggest that the Rh coverage is not grossly underestimated. (Since Rh and Pd are next to each other in the Periodic Table, their *MNN* Auger transitions are of comparable intensity, and Fig. 1 of Ref. 7 can be directly compared with Fig. 1 here. The electron beam in Ref. 7 was incident at 74° with respect to the sample normal, however, rather than 84° as stated.) The similarity between the AES results should not be taken too seriously, though, because of the obvious difference in film structure between Rh and Pd deposited on Cu(100).

Finally, the Pt coverage was also obtained by comparing the AES results with those from an ordered 50-50 surface alloy, "Cu(100)-*c*(2×2)Au," formed by deposition of 0.5 ML of Au onto Cu(100).^{6,11} (Again, since Pt and Au are next to each other in the Periodic Table, the corresponding Auger transitions are of comparable intensity.) As in the case of the comparison between Cu(100)/Rh and Cu(100)Pd, the Pt coverage obtained in this way is only approximate because of the structural differences between Pt and Au films on Cu(100).

These coverage determinations thus form the basis for the comparison made in Fig. 4 from which it is evident that (a) there is a tendency, though much greater in the case of Rh than either Pd or Pt, for Cu to remain on the surface as the film grows, and (b) the resulting film structure in all cases is metastable at 300 K in spite of the degree of relaxation which occurs spontaneously upon deposition. Roughly speaking, point (a) reflects the fact that each film-substrate combination corresponds to an unstable configuration, while (b) indicates the presence of some kinetic limitation or other barrier to the attainment of the thermodynamically preferred configuration. In order to expand on these points, it is useful to develop models for the various film structures which are consistent with other observations.

As already mentioned, the Cu(100)/Rh system appears to be rather similar to Ag(100)/Rh where, for comparable coverages and deposition rate, Rh was found to grow in a disordered layer-by-layer fashion on top of the Ag at 300 K, becoming covered with about 1 ML of Ag when heated to 600 K. Otherwise, no significant mixing of Rh and Ag was observed. The maintenance of virtually complete phase separation between Rh and Ag is consistent with the bulk phase diagram which indicates low solubilities, 0 at. % Rh and 5 at. % Ag at 475 K.¹² The negligible solubility of Rh in Ag represents a larger barrier to the incorporation of Rh atoms into Ag than Cu, however, where the corresponding solubility is moderate, 20 at. % Rh (and 5 at. % Cu) at 775 K.¹³ This could account for the different metastabilities of the Rh film against being covered by noble metal at 300 K. The film structure in

the case of Rh deposited on Cu(100) at 300 K is thus thought to consist of a partial ML (the fraction decreasing with increasing film thickness) of Cu on top of a disordered Rh-rich film on top of the Cu. The presence of dilute Rh in the underlying Cu is unlikely in view of the low bulk-diffusion rate for Rh in Cu extrapolated to this temperature.¹⁴

The Cu(100)/Pd system, on the other hand, is distinctly different from Cu(100)/Rh. It is known that the ordered 50-50 surface alloy, Cu(100)-*c*(2×2)Pd, in which Pd atoms are substituted for about half of the Cu atoms in the surface,⁹ forms below room temperature,⁷ demonstrating that adsorbed metal atoms are readily incorporated into the surface of the substrate at 300 K. Other evidence suggests that incorporation of Pd may even go somewhat beyond the surface: The Pd coverage corresponding to the best *c*(2×2) LEED pattern is 0.8 instead of 0.5 ML. In spite of this, CO chemisorption results indicate a Pd deficiency in the *c*(2×2) surface.⁷ This is also evident from Fig. 4 where it is seen that the scattering-peak amplitude for Cu is about 70% (instead of 50%) of its initial value at this coverage. Finally, the XPS results suggest that some Pd may be dissolved in the Cu below the *c*(2×2) surface. The basis for this suggestion is the seemingly larger (by 0.2–0.4 eV) Pd 3*d* core-level widths in the spectrum from the *c*(2×2) surface than in the spectrum from the thick-film alloy. That is, while in both cases the core levels are shifted (though by different amounts) relative to those of Pd due to alloying and the line shape is more symmetric than that of Pd due to the lower density of states at the Fermi level, the widths are larger in the spectrum from the *c*(2×2) surface due to relatively equal contributions from surface and bulk Pd atoms, each characterized by a different binding energy.¹⁵ The spectrum from the thick-film alloy is dominated by the contribution from bulk Pd atoms, however, and inhomogeneous broadening of this sort should not be as apparent. The initial formation of the ordered surface alloy (and possibly some bulk alloy just below the surface), consistent with the bulk phase diagram and related thermodynamic data,¹⁶ may be responsible for stabilizing the higher Pd than corresponding Rh concentration at the surface of the growing film. The film structure in the case of Pd deposited on Cu(100) at 300 K is thus thought to consist of a partially ordered, graded Cu-Pd alloy, the surface of which may be slightly enriched in Cu.

The Cu(100)/Pt system might be expected to behave like the Cu(100)/Rh system on the basis of surface energy considerations. The bulk binary phase diagrams with Cu favor an analogy between Pt and Pd, however,¹⁶ and Cu(100)/Pt indeed appears to be rather similar to Cu(100)/Pd. Thus, formation of a Cu-Pt alloy may also be responsible for stabilizing the higher Pt than corresponding Rh concentration at the surface of the growing film. While Pt apparently does not form the ordered 50-50 surface alloy found for Pd deposited on Cu(100) at 300 K, there is some indication of ordering.

The importance of alloying in controlling growth behavior, implied by these models for the various film structures, is not obvious at first glance. In the context of clas-

sical segregation theory, for example, the heats of adsorption for dilute alloys of Cu and Pt are dominated by the surface-energy contributions, as shown in Table I, constructed according to the treatment given in Ref. 17. Estimating the alloy interaction contributions for dilute alloys of Cu and Rh to be -0.4 kcal/mol,⁵ the same conclusion holds for these alloys as well, and the heats of adsorption are thus comparable to (though somewhat smaller than) those for dilute alloys of Cu and Pt. While surface segregation conditions do not apply to film growth, the heat of adsorption should provide some indication of the thermodynamic driving force appropriate to the coverage extremes corresponding to zero thickness on the one hand and finite thickness of pure film on the other. The crossover which occurs in the course of growing the film suggests an alternative way of looking at the different film-growth behavior, however, in terms of the coverage required to effect the transition. Qualitatively, the weaker tendency for Cu to remain on the surface in the case of Cu(100)/Pt than in the case of Cu(100)/Rh is just a natural consequence of the tendency for Pt to mix as opposed to the tendency for Rh to cluster upon alloy formation with Cu.

It may also be true that the surface-energy contribution to the heat of adsorption has been overestimated in Table I. In another treatment of surface segregation, using the embedded atom method, much smaller energies for solute segregation in Cu(Pd) and Cu(Pt) were obtained, possibly related to the smaller (by $\sim 60\%$) calculated surface energies for the pure materials.¹⁸ Another calculation of the surface energy of Pd, using a self-consistent, scalar-relativistic, linearized augmented Slater-type-orbital method, yielded values which are nearly the same as that used in constructing Table I, however.¹⁹ Furthermore, the segregation energies predicted for Cu(Pd) and Cu(Pt) by Ref. 18, each about 3 kcal/mol in absolute value, are of opposite sign, contrary to indications of the present experimental results.

The effect of heating films (deposited at 300 K) to 525 K is to allow additional relaxation of a nonequilibrium configuration to one of lower free energy, reflected in part by an increase in the concentration of Cu on the surface. The observation that this change takes place over nearly

the same relatively narrow temperature range for all the systems, including Ag(100)/Rh,³ suggests that a common surface diffusional process is involved. Actually, surface diffusion is understood to encompass a variety of atomic-scale processes, each characterized by a different activation energy.²⁰ Lower-energy processes are presumably responsible for the atomic rearrangements which take place upon deposition at 300 K. The extent to which these processes are ineffectual may then be indicative of the presence of relatively stable configurations, possibly clusters or islands. It is proposed that the surface compositional changes which take place upon heating to 525 K provide evidence for the existence of such configurations.

More direct evidence for these configurations can be cited in the cases of Pd and Pt. Formation of the ordered 50-50 surface alloy at 300 K in the case of Pd, for example, undoubtedly provides some stabilization against incorporation of Pd into the bulk, a process which takes place at ~ 440 K. The nearly pure Cu surface which results from heating also exhibits a good $c(2 \times 2)$ LEED pattern which may correspond to an ordered Pd-containing subsurface layer. In the case of Pt, where formation of the ordered 50-50 surface alloy does not occur at 300 K, heating also results in a nearly pure Cu surface exhibiting a good $c(2 \times 2)$ LEED pattern. The UPS results are consistent with the presence of some Pt clusters or islands upon deposition, these being responsible for Pt-derived photoemission at the Fermi level which diminishes with the more complete mixing of Pt and Cu caused by heating.

Finally, to the extent that any Rh remained on the surface for submonolayer coverages, room-temperature CO chemisorption was found to be possible. Some room-temperature CO chemisorption was also found for submonolayer coverages of Pt (but not Pd). (The presence of chemisorbed CO was detected primarily by UPS.) This is thought to be correlated with the transition-metal-derived density of states at the Fermi level indicated by the UPS results in these two cases.⁷ The Rh-derived photoemission at the Fermi level found for submonolayer coverages is consistent with electronic-structure calculations.²¹

TABLE I. Various contributions to the heat of adsorption in dilute alloys according to classical segregation theory. (The heat of adsorption is equal to surface-energy plus alloy-interaction plus strain-energy contributions.)

Alloy solvent (solute)	Surface-energy contribution (kcal/mol)	Alloy-interaction contribution (kcal/mol)	Strain-energy contribution (kcal/mol)	Heat of adsorption of solute (kcal/mol)
Rh(Cu)	-8.29	NA ^a	-2.09	
Cu(Rh)	7.85	NA	-1.29	
Pd(Cu)	-0.56	3.01	-2.31	0.14
Cu(Pd)	0.52	3.35	-2.26	1.61
Pt(Cu)	-8.24	2.29	-3.09	-9.04
Cu(Pt)	7.59	4.09	-2.94	8.74

^aNA denotes not available.

IV. CONCLUSIONS

It is concluded that surface-energy considerations correctly predict the tendency for Cu to remain on the surface as films of Rh, Pd, and Pt are grown on Cu(100) at 300 K. Properties of the bulk phases, such as clustering instead of mixing upon alloy formation, figure prominently in a closer comparison of the film-growth behaviors, however, and differences in barriers to relaxation of nonequilibrium configurations are subtle. Further refinements, such as consideration of interfacial strain energy or ordering of the compound formed, will require

considerably more detailed knowledge of the film structure.¹⁹

ACKNOWLEDGMENTS

This work has been funded, in part, by the National Science Foundation under Grant No. CHE-8451317. One of us (P.J.S.) acknowledges support from the Phillips Petroleum Company, and one of us (P.A.T.) is grateful for support from the Camille and Henry Dreyfus Foundation. We also thank R. J. Baird for use of the vacuum system in which the XPS measurements were performed and T. J. Potter for assistance in implementing the data-acquisition system.

¹E. Bauer, Appl. Surf. Sci. **11/12**, 479 (1982).

²E. Bauer, Z. Kristallogr. **110**, 372 (1958); **110**, 395 (1958).

³P. J. Schmitz, W.-Y. Leung, G. W. Graham, and P. A. Thiel, Phys. Rev. **40**, 11 477 (1989).

⁴L. Z. Mezey and J. Giber, Jpn. J. Appl. Phys. **21**, 1569 (1982).

⁵A. R. Miedema, Philips Tech. Rev. **36**, 217 (1976).

⁶G. W. Graham, Surf. Sci. **184**, 137 (1987).

⁷G. W. Graham, Surf. Sci. **171**, L432 (1986).

⁸G. C. Nelson, Sandia National Laboratories (Albuquerque, NM) Report No. SAND79-0712, 1979 (unpublished).

⁹S. C. Wu, S. H. Lu, Z. Q. Wang, C. K. C. Lok, J. Quinn, Y. S. Li, D. Tian, F. Jona, and P. M. Marcus, Phys. Rev. B **38**, 5363 (1988).

¹⁰G. W. Graham, J. Vac. Sci. Technol. A **4**, 760 (1986).

¹¹Z. Q. Wang, Y. S. Li, C. K. C. Lok, J. Quinn, F. Jona, and P. M. Marcus, Solid State Commun. **62**, 181 (1987).

¹²I. Karakaya and W. T. Thompson, Bull. Alloy Phase Diagrams **7**, 362 (1986).

¹³D. J. Chakrabarti and D. E. Laughlin, Bull. Alloy Phase Diagrams **2**, 460 (1982).

¹⁴D. B. Butrymowicz, J. R. Manning, and M. E. Read, *Diffusion Rate Data and Mass Transport Phenomena for Copper Systems*, INCRA Monograph Series V (International Copper Research Association, New York, 1977), pp. 250 and 251.

¹⁵G. W. Graham, J. Vac. Sci. Technol. A **5**, 631 (1987).

¹⁶R. Hultgren and P. D. Desai, *Selected Thermodynamic Values and Phase Diagrams for Copper and Some of its Binary Alloys*, INCRA Monograph Series I (International Copper Research Association, New York, 1971), pp. 136–148.

¹⁷P. Wynblatt and R. Ku, in *Interfacial Segregation*, edited by W. C. Johnson and J. M. Blakely (American Society for Metals, Metals Park, OH, 1979), pp. 115–136.

¹⁸S. M. Foiles, M. I. Baskes, and M. S. Daw, Phys. Rev. B **33**, 7983 (1986).

¹⁹M. Weinert, R. E. Watson, J. W. Davenport, and G. W. Fernando, Phys. Rev. B **39**, 12 585 (1989).

²⁰W. F. Egelhoff, J. Vac. Sci. Technol. A **7**, 2060 (1989).

²¹J. Kudrnovshy and V. Drchal, Solid State Commun. **65**, 613 (1988).